Electronic structure of hole-doped Co-Fe cyanides: $Na_{1.60-\delta}Co[Fe(CN)_6]_{0.90}\cdot 2.9H_2O$ $(0.0\leq\delta\leq 0.85)$

K. Igarashi, F. Nakada, and Y. Moritomo*
Department of Physics, University of Tsukuba, Tsukuba 305-8571, Japan
(Received 18 August 2008; published 5 December 2008)

Lattice, magnetic, and optical properties are investigated for films of Prussian-blue-type cyanides, $Na_{1.60-\delta}Co[Fe(CN)_6]_{0.90}\cdot 2.9H_2O$ $(0.0\leq\delta\leq 0.85)$, as a function of hole concentration δ of the *d*-electron system. The mother compound $(\delta=0)$ takes the Co^{2+} $(t_{2g}^5e_g^2:S=3/2)$-Fe^{2+} $(t_{2g}^6:S=0)$ configuration, and the holes are selectively introduced on the Co site. We found that effective magnetic moment $\mu_{\rm eff}$ decreases with δ, indicating that the Co^{3+} ion takes a low-spin state $(t_{2g}^6:S=0)$. Visible absorption spectra are dominated by three absorption bands at $\approx$2.2 eV, $\approx$3.3 eV, and $\approx$3.8 eV, which are ascribed to charge transfer from Fe^{2+} to Co^{3+} sites, CN^- to Fe^{2+} sites, and CN^- to Co^{3+} sites, respectively. Based on these assignments, we proposed an electronic structure model. We further comprehensively discuss variation in the electronic structure with change in the transition-metal site.

DOI: 10.1103/PhysRevB.78.235106 PACS number(s): 81.30.Dz, 78.66.Nk, 74.62.Bf, 81.05.Rm

I. INTRODUCTION

The hole-doping procedure frequently contributes to a deeper comprehension of the strongly correlated electron systems and to material design for realization of unconventional physical properties as well as giant response to external stimuli.[1] The hole doping is possible in the Prussian-blue-type cyano-bridged transition-metal compound, $A_xM[Fe(CN)_6]_y\cdot zH_2O$ (*A* and *M* are alkaline metal and transition metal, respectively),[2,3] by means of the electrochemical method.[4,5] Crystallographically, the compounds belong to the face-centered cubic ($Fm\bar{3}m$; $Z=4$ or $F\bar{4}3m$; $Z=4$), in which two transition metals form a rock-salt-type (NaCl-type) network with sharing cyano (CN^-) moieties, -CN-*M*-NC-Fe-CN-*M*-.[6] Nanospaces within the network accommodate the alkaline metal ions (A^+) and some water molecules (zerolite water). The residual water molecules (ligand water) occupy the vacancy of the $[Fe(CN)_6]$ site and coordinate to the *M* site. We can remove *A* from the nanospaces by an electrochemical method, and introduce the holes on the *d*-electron system. In the $Na_{0.72-\delta}Ni[Fe(CN)_6]_{0.68}\cdot 5.1H_2O$ system,[3] the hole doping at the Fe site induces ferromagnetic transition at $\delta=0.26$, and the transition temperature T_C increases from 11 K at $\delta=0.26$ to 21 K at $\delta=0.58$. Thus, hole doping is a powerful tool to control the material properties in the Prussian-blue-type compounds.

So far, Nakada *et al.*[2] and Shibata *et al.*[3] have investigated the electronic structure by visible absorption spectra of the hole-doped Ni-Fe system $(Na_{0.72-\delta}Ni[Fe(CN)_6]_{0.68}\cdot 5.1H_2O)$ and the hole-doped Co-Fe system $(Na_{0.84-\delta}Co[Fe(CN)_6]_{0.71}\cdot 3.8H_2O)$. In these systems, the holes are introduced on the Fe site, and the electronic configuration of the network is expressed as M^{2+}-$Fe^{2+\delta}$.[7] On the other hand, the Prussian blue, i.e., $Fe^{III}[Fe^{II}(CN)_6]_{3/4}\cdot 3.5H_2O$, takes an opposite electronic configuration: the *M* site takes a trivalent state, or the holes are introduced on the *M* site. Then, it is significant to comprehensively understand the variation in the electronic structure with change in the *M* site (*M*=Fe, Co, and Ni), similar to the case of the perovskite-type oxides $(La,Y)MO_3$ (Refs. 8 and 9) and $LaSrMO_4$.[10]

Among the Prussian-blue compounds, the Co-Fe system shows characteristic electronic properties. Its electronic configuration can be controlled by the concentration of the $[Fe(CN)_6]$ vacancy $(1-y)$: the Fe site takes a trivalent state at $y=0.67-0.75$ at 300 K, while the Co site takes a trivalent at $y=0.86$.[11] The variation in the electronic configuration is ascribed to the ligand field effect around the Co site.[2,11] In the large-*y* compound, the enhanced ligand field stabilizes the low-spin Co^{3+} (t_{2g}^6) state. Recently, Kamioka *et al.*[12] investigated dynamics of the charge-transferred state in Prussian-blue-type cyanide.[12,13] Especially, in $Co^{II}[Fe^{III}(CN)_6]_{2/3}5H_2O$, they found that lifetime τ_{CT} of the charge-transferred state at 10 K elongates as absorbed photon density *n* increases. This observation suggests an attractive interaction between the charge-transferred sites, which may cause a *hidden* phase.

In this paper, we have investigated the electronic structure of the hole-doped Co-Fe system with large *y*, films of $Na_{1.60-\delta}Co[Fe(CN)_6]_{0.90}\cdot 2.9H_2O$ $(0.0\leq\delta\leq 0.85)$, whose electronic configuration is expressed as $Co^{2+\delta}$-Fe^{2+}. Based on systematic investigation of visible absorption spectra against δ, we assigned absorption bands in the visible-violet region and proposed an electronic structure model. We comprehensively discuss variation in the electronic structure with change in the transition-metal site.

II. EXPERIMENTAL

A. Sample preparation and characterization

Films of $Na_xCo[Fe(CN)_6]_y\cdot zH_2O$ were electrochemically synthesized on ITO transparent electrodes (sheet resistance was 100 Ω) under potentiostatic conditions at −0.5 V versus a standard Ag/AgCl electrode in an aqueous solution containing 0.8 mmol/L $K_3[Fe^{III}(CN)_6]$, 0.5 mmol/L $Co^{II}(NO_3)_2$, and 5 mol/L $Na(NO_3)$. We added saw-toothed-type modulation (±0.35 V and 71 Hz) to the applied potential, which enhances the ⟨111⟩ orientation.[2] Before the film growth, the surface of the ITO electrode was purified by electrolysis of water for several minutes. The obtained films

were of transparent green. Elemental analysis by the inductively coupled plasma (ICP) method and a CNH organic elementary analyzer (Perkin-Elmer 2400 CNH Elemental Analyzer) yields $Na_{1.60}Co[Fe(CN)_6]_{0.90}\cdot 2.9H_2O$. The film thickness was ~1000 nm, which was determined by the cross-sectional image of a scanning electron microscope (SEM).

Hole concentration δ of the film was controlled by the oxidization of the film at 0.4–0.6 V versus a standard Ag/AgCl electrode in 0.5 mol $Na(NO_3)$ aqueous solution. X-ray diffraction patterns of the valence-controlled films were measured in the $\theta-2\theta$ geometry. Observed reflections can be indexed with the face-centered cubic cell.

B. Magnetic measurement

Magnetic properties of the hole-doped films were investigated with a SQUID magnetometer (Quantum Design MPMS). In order to reduce background magnetic susceptibility, the film was carefully removed from the ITO glass with a microspatula, and the fine powders were filled into a 0.5 mm ϕ glass capillary. The typical sample mass was ~100 μg. The background signal from the glass capillary is on the order of 10^{-6} emu, which is 2 orders smaller than the signal from the sample powders. We were careful enough to seal the glass capillary to keep the circumstance.

C. Optical measurement

Absorption spectra in the infrared region were measured with use of an infrared microscope system (JASCO ITR-3000) equipped with a Fourier-transform type infrared spectrometer (FT-IR). Transmitted light was focused on a cooled MCT (HgCdTe) infrared detector. We posted Scotch tape on the film surface to reduce the interference effect. Absorption spectra in the visible-violet region were measured with a conventional monochrometer system with a halogen lamp. The transmitted light was focused on a Si-photodiode, and a lock-in detection was adopted to improve the S/N ratio.

III. RESULTS

A. Valence control by an electrochemical method

We plotted in Fig. 1 the chemical composition of $Na_xCo[Fe(CN)_6]_y\cdot zH_2O$, that is, x, y, and z, as a function of the total charge q used in the oxidization process. x linearly decreases with q as $x=1.60-0.98q$. So, we used the empirical relation between q and x to estimate δ $(=1.60-x)$. We emphasize that y (=0.90) and z (=2.9) are nearly constant and are independent of δ. Here, note that the parameter δ represents the concentration of the trivalent transition metal per Co site: $Na_{1.60-\delta}Co[Fe(CN)_6]_{0.90}\cdot 2.9H_2O$ can be expressed as $Na^{I}_{1.60-\delta}Co^{II}_{1-\delta}Co^{III}_{\delta}[Fe^{II}(CN)_6]\cdot 2.9H_2O$.

Figure 2 shows infrared absorption spectra of the films at 300 K. In the as-grown film ($\delta=0.00$), an intense absorption band is observed at 2087 cm^{-1}, which is ascribed to the stretching vibration mode of the CN moiety in the $[Fe^{II}(CN)_6]$ complex.[14] The CN stretching mode shows a blueshift with an increase in δ. The blueshift is ascribed to decrease in the lattice constant a: $a=10.4$ Å at $\delta=0.0$ and

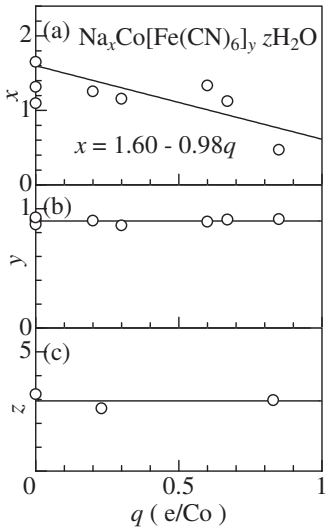

FIG. 1. Chemical composition of $Na_xCo[Fe(CN)_6]_y\cdot zH_2O$ films against the total charge q used in the oxidization process: (a) x, (b) y, and (c) z. The chemical composition was determined by the elemental analysis by the ICP method and a CNH organic elementary analyzer.

$a=10.0$ Å at $\delta=0.85$ [see Fig. 5(b)]. The band finally reaches 2121 cm^{-1} at $\delta=0.85$, which is close to the energy $(=2122\ cm^{-1})$ of the Fe^{2+}-CN-Co^{3+} band in bulk $Na_{0.81}Co[Fe(CN)_6]_{0.86}\ 2.6H_2O$.[11] In Fig. 3, we plotted the energy E_{CN} and the oscillator strength f against δ. The magnitude of E_{CN} linearly increases with δ, showing an amalgamation behavior: $E_{CN}[cm^{-1}]=2086+43\delta$. This amalgamation behavior in the present system makes a sharp contrast with the persistent behavior observed in $Na_{0.84-\delta}Co[Fe(CN)_6]_{0.71}\cdot 3.8H_2O$ system.[2] This clearly indicates that the holes are introduced on the Co site. On the other hand, the magnitude of f is nearly constant $(=0.03/Fe)$.

B. Spin state of Co

Now, let us proceed to the magnetic properties of thin films of $Na_{1.60-\delta}Co[Fe(CN)_6]_{0.90}\cdot 2.9H_2O$. In Fig. 4, we show δ dependence of the magnetic susceptibility χ, which was obtained in the cooling run under a magnetic field of 5000 gauss. In the entire concentration range, the χ-T curves show the Curie-Weiss behavior. So, we analyzed the χ-T curves with the function

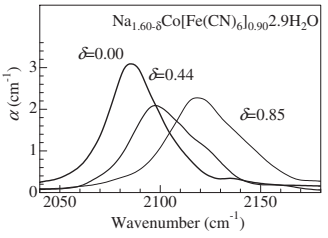

FIG. 2. Infrared absorption spectra of thin films of $Na_{1.60-\delta}Co[Fe(CN)_6]_{0.90}\cdot 2.9H_2O$ measured at 300 K at different doping levels.

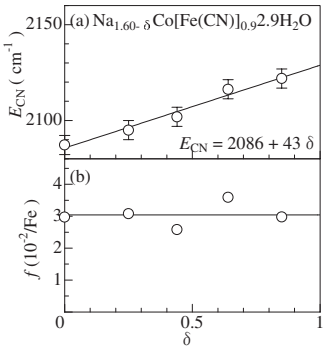

FIG. 3. Energy E_{CT} and oscillator strength f of the CN stretching vibration of thin films of $Na_{1.60-\delta}Co[Fe(CN)_6]_{0.90}\cdot 2.9H_2O$ at 300 K. The straight lines are the least-square-fitted results.

$$\chi = \frac{C}{T + T_{CW}} + \chi_0, \tag{1}$$

where C, T_{CW}, and χ_0 are the Curie constant, the Weiss temperature, and the background susceptibility, respectively. The least-square fitting was performed in the temperature range from 50 to 300 K. Thus obtained μ_{eff} is plotted in Fig. 5(a) against δ. At $\delta=0.0$, the magnitude of μ_{eff} (=4.25 μ_B/Co) is close to the ideal value (=3.87 μ_B/Co) for high-spin Co^{2+} ($t_{2g}^5 e_g^2$; $S=3/2$). If the Co^{3+} ions take the low-spin state ($S=0$), the density of the spin species (Co^{2+}) is $1-\delta$ in the intermediate-δ region. Then, the magnitude of $\mu_{eff}(\delta)$ is expressed as

$$\mu_{eff}(\delta) = \sqrt{15(1-\delta)}. \tag{2}$$

This model well reproduces the experimentally obtained μ_{eff}, as indicated by the solid curve in Fig. 5(a).

In Fig. 5(b), we show δ dependence of the lattice constant a. The magnitude of a linearly decreases with δ as a[Å] $=10.38-0.40\delta$. Such a reduction in a is quantitatively understood in terms of the ionic radius r_{Co} of the Co ion. The hole-doping procedure reduces r_{Co} from 0.745 Å for the high-spin Co^{2+} ($\delta=0$) to 0.545 Å for the low-spin Co^{3+}

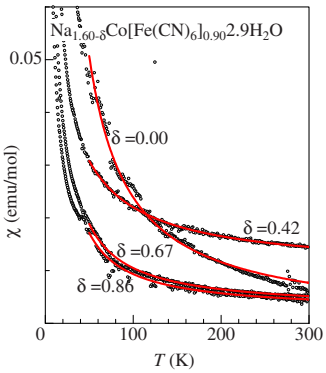

FIG. 4. (Color online) Temperature dependence of the magnetic susceptibility χ of $Na_{1.60-\delta}Co[Fe(CN)_6]_{0.90}\cdot 2.9H_2O$. The data points were obtained in the cooling run under a magnetic field of 5000 gauss. Solid curves are the results of the least-square fitting (see text).

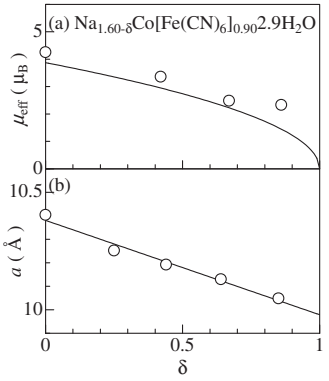

FIG. 5. (a) Effective magnetic moment μ_{eff} of $Na_{1.60-\delta}Co[Fe(CN)_6]_{0.90}\cdot 2.9H_2O$ against δ. The solid curve is the calculation (see text). (b) Lattice constant a at 300 K against δ. The solid line is the least-square-fitting result.

($\delta=1$).[15] Then, the reduction Δa of the lattice constant is expected to be 0.40 Å (=$2\Delta r_{Co}$), which agrees with the experiment (=0.40 Å).

C. Visible absorption spectra

Figure 6 shows the visible absorption spectra of the films at 300 K: (a) $\delta=0.00$, (b) $\delta=0.44$, and (c) $\delta=0.85$. In the as-grown film [(a) $\delta=0.00$], an intense absorption band is observed at 3.3 eV (A band) together with the weak absorptions around 2 eV (Co^{II} band). The Co^{II} bands are ascribed to the intra-atomic d-d transition of Co^{2+}.[2] The absorption spectrum of the fully hole-doped sample [(c) $\delta=0.85$] is dominated by three components observed at ≈2.2 eV (CT band), ≈3.3 eV (A band), and ≈3.8 eV (B band). Among them, the lowest-lying band (CT band) is ascribed the charge transfer from the Fe^{2+} site to the Co^{3+} site.[2,11] We decomposed the

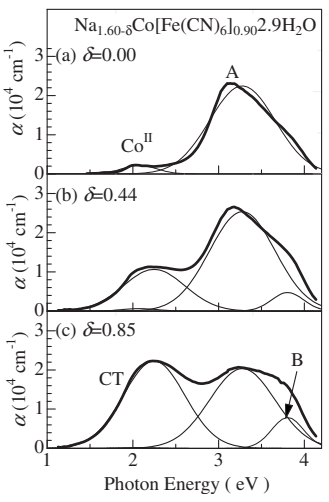

FIG. 6. Absorption spectra of thin films of $Na_{1.60-\delta}Co[Fe(CN)_6]_{0.90}\cdot 2.9H_2O$ measured at 300 K: (a) $\delta=0.00$, (b) $\delta=0.44$, and (c) $\delta=0.85$. The thin curves represent the least-square fitting with the four gauss-type components (the Co^{II}, A, B, and CT bands: see text). Co^{II} bands are ascribed to the intra-atomic d-d transition of Co^{2+}.

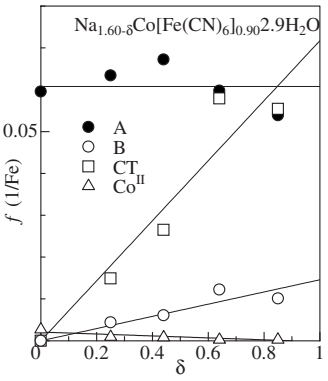

FIG. 7. Oscillator strength f of thin films of $Na_{1.60-\delta}Co[Fe(CN)_6]_{0.90}\cdot 2.9H_2O$ at 300 K. The straight lines are the least-square-fitted results.

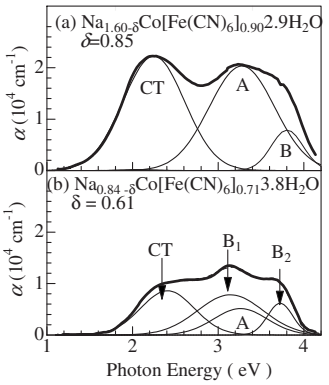

FIG. 8. Room-temperature absorption spectra of thin films of (a) $Na_{1.60-\delta}Co[Fe(CN)_6]_{0.90}\cdot 2.9H_2O$ (δ=0.85) and (b) $Na_{0.84-\delta}Co[Fe(CN)_6]_{0.71}\cdot 3.8H_2O$ (δ=0.61: cited from Ref. 2). Holes are introduced on the Co (Fe) site in the former (latter) compound.

absorption spectra $\alpha(\omega)$ into four components:

$$\alpha(\omega) = \sum_{i=\mathrm{A,B,CT,Co^{II}}} \frac{S_i}{\pi^{1/2}\Gamma_i} \exp\left(-\frac{(\hbar\omega_i - \hbar\omega)^2}{\Gamma_i^2}\right), \qquad (3)$$

where S_i, $\hbar\omega_i$, and Γ_i are the spectral weight, the resonant energy, and the spectral width, respectively. In the fitting procedure, we fixed values of $\hbar\omega_i$ and W_i and adjusted only the magnitude of S_i. The thin solid curves in Fig. 6 are the least-square-fitted results.

In Fig. 7, we plotted the oscillator strength f of the respective components against δ. The magnitude of f of the A band is almost constant, indicating that the band has no relation with the Co site. This behavior is consistent with the assignment of the A band, that is, intermolecular transition of $[Fe^{2+}(CN)_6]$. Magnitude of f of the Co^{II} band linearly decreases with δ, which is consistent with the assignment, that is, the intra-atomic d-d transition of Co^{2+}. On the other hand, magnitude of f of the B and CT bands linearly increase with δ, indicating that these bands are related with the Co^{3+} species. This behavior is consistent with the assignment of the CT band, that is, $Fe^{2+} \rightarrow Co^{3+}$. We ascribed the B bands to the charge transfer from the CN^- site to the Co^{3+} site. In Table I, we listed the parameters of the optical transitions together with the assignment. We note that the magnitude of f (=0.08/Fe) for the CT transition is comparable to that (=0.03/Mn) for the J-gap transition (electron transfer between the neighboring Mn sites) in $La_{0.6}Sr_{0.4}MnO_3$.[16]

TABLE I. Resonance energy $\hbar\omega$; oscillator strength f of the optical transitions of $Na_{1.60-\delta}Co[Fe(CN)_6]_{0.90}\cdot 2.9H_2O$.

Transition	$\hbar\omega$ (eV)	f	Assignment
A	3.28	0.07/Fe^{2+}	$CN^- \rightarrow Fe^{2+}$
B	3.80	0.01/Co^{3+}	$CN^- \rightarrow Co^{3+}$
CT	2.25	0.08/Co^{3+}	$Fe^{2+} \rightarrow Co^{3+}$
Co^{II}	2.08	0.002/Co	d-d within Co^{2+}

IV. DISCUSSION

A. Comparison with Co^{2+}-$Fe^{2+\delta}$ system

Let us compare the electronic structure of the present $Co^{2+\delta}$-Fe^{2+} system with the Co^{2+}-$Fe^{2+\delta}$ system. In Fig. 8, we compare absorption spectra of (a) $Na_{1.60-\delta}Co[Fe(CN)_6]_{0.90}\cdot 2.9H_2O$ (δ=0.85) and (b) $Na_{0.84-\delta}Co[Fe(CN)_6]_{0.71}\cdot 3.8H_2O$ (δ=0.61). Holes are introduced on the Co (Fe) site in the former (latter) compound. As discussed in the previous section, the absorption spectrum of the $Co^{2+\delta}$-Fe^{2+} system [Fig. 8(a)] is dominated by the A, B, and CT bands. In the Co^{2+}-$Fe^{2+\delta}$ system [Fig. 8(b)], the spectrum is dominated by the A, B_1, B_2, and CT bands.[2] The A band due to the intermolecular transition of $[Fe^{2+}(CN)_6]$ is observed at $\approx$3.3 eV for both the systems, indicating that the local electronic states of $[Fe^{2+}(CN)_6]$ are nearly the same. On the other hand, the energy of the CT band in Fig. 8(a) is $\approx$0.1 eV lower than that of the CT band in Fig. 8(b). The B_1 and B_2 bands in Fig. 8(a) are ascribed to charge transfer from CN^- to the hole-doped site, that is, low-spin Fe^{3+} (t_{2g}^5) sites. The doublet structure is due to the unoccupied t_{2g} state of Fe^{3+}. The corresponding component in Fig. 8(a) is the B band, which is ascribed to the charge transfer from CN^- to low-spin Co^{3+} (t_{2g}^6). Note that the doublet structure is absent, since the t_{2g} state is fully occupied in Co^{3+}.

In Fig. 9, we schematically show the electronic structures of (a) the $Co^{2+\delta}$-Fe^{2+} system and (b) the Co^{2+}-$Fe^{2+\delta}$ system. We fixed the energy levels of the ligand state (L^-) and Fe d_6 states, because the position of the A band ($CN^- \rightarrow Fe^{2+}$) is nearly the same for both the systems. In the nondoped (δ=0) compound, the energy levels of the Fe d_6 state and Co d_7 state are nearly degenerated. Then, slight modification of the ligand field around the Co site can reverse the levels. In the small-y system [Fig. 8(b)], the Co d_7 state is barely stable than the Fe d_6 state. On the other hand, in the present large-y system [Fig. 8(a)], the enhanced ligand field unstabilizes the Co d_7 ($t_{2g}^5 e_g^2$) state to reverse the levels. Here, we comment that the electron-lattice interaction plays a significant role in the stabilization of the Co d_7 state. Yokoyama *et al.*[17] investigated bond distance of the Co-Fe cyanides by x-ray absorp-

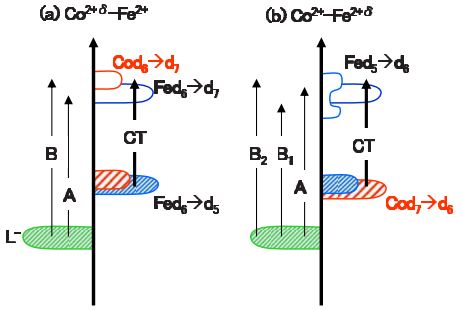

FIG. 9. (Color online) Electronic structure of (a) $Co^{2+\delta}$-Fe^{2+} and (b) Co^{2+}-$Fe^{2+\delta}$. L^- represents ligand CN^-. Impurity Fe d_5 state has a fine structure reflecting the unoccupied t_{2g} state. Vertical arrows indicate the optical transitions (see text).

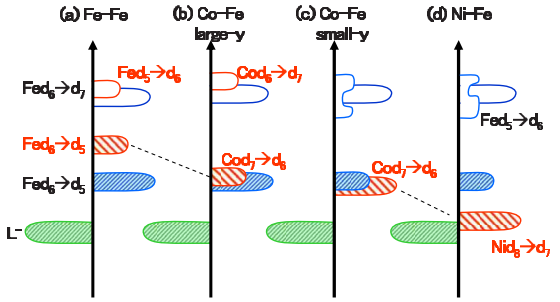

FIG. 10. (Color online) Electronic structure of (a) Fe-Fe system, (b) Co-Fe system with large y, (c) Co-Fe system with small y, and (d) Ni-Fe system. L^- represents ligand CN^-. The broken line indicates stabilization of the divalent M state with d-electron number.

tion spectroscopy, and found that the Co^{III}-N bond distance ($\approx$1.9 Å) is much shorter than the Co^{II}-N bond distance ($\approx$2.1 Å). Such a contraction in the bond distance further enhances the ligand field around the Co site. In the hole-doped compound, impurity states, i.e., Co d_6 state (Fe d_5 state) in the $Co^{2+\delta}$-Fe^{2+} (Co^{2+}-$Fe^{2+\delta}$) system, appear above the Fermi level E_F. These electronic structures well explain the observed absorption bands as indicated by arrows in Figs. 8(a) and 8(b).

B. Variation in electronic structure in *M*-Fe system

Finally, let us discuss variation in the electronic structure with change in the M site (M=Fe, Co, and Ni). We schematically show the above-discussed electronic structure model for the M-Fe system: (a) Fe-Fe system, (b) Co-Fe system with large y, (c) Co-Fe system with small y, and (d) Ni-Fe system. Similar to the above discussion, we fixed energy levels of L^-, Fe d_6 state, and impurity Fe d_5 state. On the other hand, the energy level of the divalent M state is lowered as the d-electron number increases from Fe d_6 and Co d_7 to Ni d_8, as indicated by the broken line in Fig. 10. In the Fe-Fe system, the Fe d_6 state locates higher than the Fe d_6 state of the $[Fe(CN)_6]$ complex, which well explains the formal valence of the Prussian blue, $Fe^{III}[Fe^{II}(CN)_6]_{3/4}\cdot 3.5H_2O$. In the Ni-Fe system, the Ni d_8 state locates lower than the Fe d_6 state, which is consistent with the fact that holes are introduced on the Fe site in $Na_{0.72-\delta}Ni[Fe(CN)_6]_{0.68}\cdot 5.1H_2O$.[3]

The electronic structure model shown in Fig. 10 further explains overall features of the absorption spectra of the M-Fe system. In $Fe^{III}[Fe^{II}(CN)_6]_{3/4}\cdot 3.5H_2O$, an intense absorption band is observed at 1.8 eV,[13] which is ascribed to charge transfer from the Fe^{2+} site of the $[Fe(CN)_6]$ complex to the high-spin Fe^{3+} site. In the model [Fig. 10(a)], the optical transition corresponds to the procedure to remove an electron from the original Fe d_6 state and to add an electron to the impurity Fe d_5 state. Here note that the oscillator strength of the Mott transition, i.e., removal of an electron from the impurity Fe d_6 state and addition of an electron to the impurity Fe d_6 state, is fairly weak in the Prussian-blue compound, in which two transition metals form a rock-salt-type network with sharing the CN^- moieties. In the Co-Fe system, charge-transfer excitation from the Fe^{2+} site to the Co^{3+} site (from the Co^{2+} site to the Fe^{3+} site) is observed at 2.3 eV (2.4 eV), as seen in Fig. 8(a) [Fig. 8(b)]. The optical transition corresponds to the procedure as indicated by an arrow in Fig. 9(a) [Fig. 9(b)]. In the Ni-Fe system, charge-transfer excitation from the Ni^{2+} site to the Fe^{3+} site is absent and/or overlapped with the intense ligand-to-metal absorptions.[3] This is consistent with the electronic structure shown in Fig. 10(d).

V. SUMMARY

We have investigated the electronic structure of the hole-doped Co-Fe system with large y, films of $Na_{1.60-\delta}Co[Fe(CN)_6]_{0.90}\cdot 2.9H_2O$ ($0.0 \leq \delta \leq 0.85$). Based on the δ dependence of the visible absorption spectra, we proposed an electronic structure model. Our model well explains the overall features of the electronic configuration as well as the absorption spectra of the M-Fe system (M=Fe, Co, and Ni). We believe that the electronic structure is a good starting point to comprehend the electronic properties of the Prussian-blue-type compound.

ACKNOWLEDGMENTS

This work was supported by a Grant-In-Aid for Scientific Research from the Ministry of Education, Culture, Sports, Science and Technology of Japan and the Support Center for Advanced Telecommunication (SCAT) Foundation.

*Author to whom correspondence should be addressed.

[1] For example, see Y. Tokura and N. Nagaosa, Science **288**, 462 (2000).

[2] F. Nakada, H. Kamioka, Y. Moritomo, J. E. Kim, and M. Takata, Phys. Rev. B **77**, 224436 (2008).

[3] T. Shibata, F. Nakada, H. Kamioka, and Y. Moritomo, J. Phys. Soc. Jpn. **77**, 104714 (2008).

[4] K. Itaya, I. Uchida, and D. V. Neff, Acc. Chem. Res. **19**, 162

(1986).
[5] O. Sato, Y. Einaga, T. Iyoda, A. Fujishima, and K. Hashimoto, J. Phys. Chem. B **101**, 3903 (1997).
[6] H. J. Buser, D. Schwarzenbach, W. Petter, and A. Ludi, Inorg. Chem. **16**, 2704 (1977).
[7] The parameter δ represents the concentration of the trivalent Fe site per Co site:

$$Na_{0.72-\delta}Ni[Fe(CN)_6]_{0.68} \cdot 5.1H_2O$$

$(Na_{0.84-\delta}Co[Fe(CN)_6]_{0.71} \cdot 3.8H_2O)$ can be expressed as

$$Na^{I}_{0.72-\delta}Ni^{II}[Fe^{II}(CN)_6]_{0.68-\delta}[Fe^{III}(CN)_6]_{\delta} \cdot 5.1H_2O$$

$$(Na^{I}_{0.84-\delta}Ni^{II}[Fe^{II}(CN)_6]_{0.71-\delta}[Fe^{III}(CN)_6]_{\delta} \cdot 3.8H_2O).$$

[8] T. Arima, Y. Tokura, and J. B. Torrance, Phys. Rev. B **48**, 17006 (1993).
[9] T. Arima and J. Tokura, J. Phys. Soc. Jpn. **64**, 2488 (1995).
[10] Y. Moritomo, T. Arima, and Y. Tokura, J. Phys. Soc. Jpn. **64**, 4117 (1995).
[11] N. Shimamoto, S. Ohkoshi, O. Sato, and K. Hashimoto, Inorg. Chem. **41**, 678 (2002).
[12] H. Kamioka, Y. Moritomo, W. Kosaka, and S. Ohkoshi, Phys. Rev. B, **77**, 180301(R) (2008).
[13] H. Kamioka, Y. Moritomo, W. Kosaka, and S. Ohkoshi, J. Phys. Soc. Jpn. **77**, 093710 (2008).
[14] E. Reguera, J. F. Bertran, C. Diaz, and J. Blanco, Hyperfine Interact. **53**, 391 (1990).
[15] R. D. Shannon, Acta Crystallogr., Sect. A: Cryst. Phys., Diffr., Theor. Gen. Crystallogr. **32**, 751 (1976).
[16] Y. Moritomo, A. Machida, K. Matsuda, M. Ichida, and A. Nakamura, Phys. Rev. B **56**, 5088 (1997).
[17] T. Yokoyama, T. Ohta, O. Sato, and K. Hashimoto, Phys. Rev. B **58**, 8257 (1998).